Eur Biophys J (2001) 29: 607–620
DOI 10.1007/s002490000109

ARTICLE

**Wolfgang J. Parak · Michael George · Michael Kudera**
**Hermann E. Gaub · Jan C. Behrends**

# Effects of semiconductor substrate and glia-free culture on the development of voltage-dependent currents in rat striatal neurones

Received: 7 April 2000 / Revised version: 19 May 2000 / Accepted: 18 August 2000 / Published online: 14 November 2000


**Abstract** An essential requirement for successful long-term coupling between neuronal assemblies and semiconductor devices is that the neurones must be able to fully develop their electrogenic repertoire when growing on semiconductor (silicon) substrates. While it has for some time been known that neurones may be cultured on silicon wafers insulated with $SiO_2$ and $Si_3N_4$, an electrophysiological characterisation of their development under such conditions is lacking. The development of voltage-dependent membrane currents, especially of the rapid sodium inward current underlying the action potential, is of particular importance because the conductance change during the action potential determines the quality of cell-semiconductor coupling. We have cultured rat striatal neurones on either glass coverslips or silicon wafers insulated with $SiO_2$ and $Si_3N_4$ using both serum-containing and serum-free media. We here report evidence that not only serum-free culture media but also growth on semiconductor surfaces may negatively affect the development of voltage-dependent currents in neurones. Furthermore, using surface-charge measurements with the atomic force microscope, we demonstrate a reduced negativity of the semiconductor surface compared to glass. The reduced surface charge may affect cellular development through an effect on the binding and/or orientation of extracellular matrix proteins, such as laminin. Our findings therefore suggest that semiconductor substrates are not entirely equivalent to glass in terms of their effects on neuronal cell growth and differentiation.

J.C. Behrends (✉)
Center for Nanoscience and Department of Physiology,
University of Munich, Pettenkoferstrasse 12,
80336 Munich, Germany
E-mail: j.behrends@lrz.uni-muenchen.de
Tel.: +49-89-5996248
Fax: +49-89-5996216

W.J. Parak · M. George · M. Kudera · H.E. Gaub
Center for Nanoscience and Department of Applied Physics
and Biophysics, University of Munich,
Amalienstrasse 54, 80799 Munich, Germany

**Key words** Semiconductor · Culture · Development · Inward current · Outward current

## Introduction

Neurone-semiconductor hybrids for non-invasive, simultaneous detection of the impulses of multiple single neurones in a network may lead to the development of new integrated bio-electronic devices with very useful properties for both experimental and medical applications (Bergveld 1970; Gross et al. 1977, 1997; Vassanelli and Fromherz 1998). A problem of key importance in the construction of such devices is the preservation and/or optimisation of those properties that govern the efficacy of electrical coupling between the neurone and the semiconducting material (Parak et al. 1999). Arguably, the most important of these properties on the neurone's side is transmembrane current flow during the action potential. Regardless of the detection principle employed, in order to enable detection by the semiconductor device, the action current should be as large and as rapid as possible to maximise both resistive and capacitive coupling.

In previous attempts at neurone-semiconductor coupling, culture conditions have been chosen to optimise the contact between neurones and the substrate. For instance, serum-free media, such as B27-supplemented neurobasal medium [NMB (Brewer et al. 1993; Brewer 1995; Evans et al. 1998)], have been used to suppress the growth of glial cells, which may otherwise prevent direct contact between neurones and the substrate (Offenhäusser et al. 1997). Furthermore, in order to promote cell adhesion (Offenhäusser and Rühe 1995), substrates have generally been coated with laminin (Lamoureux et al. 1992; Matsuzawa et al. 1997; Offenhäusser et al. 1997). While it has been shown that both embryonic and adult nerve cells in serum-free culture retain a neuronal phenotype electrophysiologically (Evans et al. 1998), there is scant information available to date as to the development of the electrogenic prop-

erties of neurones cultured on semiconductor surfaces under these conditions compared with more traditional culture protocols. Lacking in particular is a quantitative and direct comparison of the time-dependence of in vitro development of electrogenesis in glia-free versus neuroglial cultures on conventional (glass) and semiconductor substrates.

Neurones in culture acquire full excitability over several days of development (MacDermott and Westbrook 1986; Gottmann et al. 1988; Kowalski et al. 1995). We have studied the development of electrogenesis in rat striatal neurones prepared from E17 foetal rat brains plated onto either glass coverslips or insulated Si wafers using both serum-containing medium (SCM) and serum-free NBM. In the present study, we find that the density of the voltage-dependent inward current, largely carried by $Na^+$ ions, is severely reduced in neurones grown in NBM with respect to those developing as neuroglial cocultures in SCM. More surprisingly, in SCM the development of the inward current is also significantly slowed down in neurones growing on silicon substrates with respect to those growing on glass. We also found significant differences between Si wafers and glass in the developmental pattern of outward ($K^+$) conductance expression. Thus, our results show that there is considerable room for improvement in culture conditions in order to optimise the contact between neurones and semiconductors. In addition, despite the electrochemical similarity of glass and $Si_3N_4/SiO_2$ surfaces, our findings suggest that, for the purpose of neural cell culture, important differences may exist between glass and $Si_3N_4/SiO_2$ in the properties of the resulting electrolyte-insulator interface. Specifically, charge measurements using the atomic force microscope demonstrate a reduced negativity of semiconductor surfaces with respect to glass that may influence neuronal development via interaction with extracellular matrix proteins used to promote cell adhesion.

## Materials and methods

### Cultures and electrophysiological techniques

Dissociated striatal neurones were obtained from E17 rat foetuses as described previously (Rumpel and Behrends 1999). All efforts were made to minimise animal suffering and to reduce the number of animals used. Cells were cultured either on semiconductor substrates (silicon wafers insulated with a thermally grown 20-nm layer of $SiO_2$ on which 50 nm of $Si_3N_4$ were deposited by chemical vapor deposition, supplied by Prof. I. Eisele, Universität der Bundeswehr, Neubiberg, Germany) or on glass coverslips (Assistent, Munich, Germany) made of Schott D263M glass containing 64.1% $SiO_2$, 8.4% $B_2O_3$, 4.2% $Al_2O_3$, 6.4% $Na_2O$, 6.9% $K_2O$, 5.9% ZnO, 4.0% $TiO_2$ and 0.1% $Sb_2O_3$. The additional insulation of semiconductor devices with $Si_3N_4$ is necessary to prevent the diffusion of $Na^+$ ions through the $SiO_2$ into the Si wafer (Yon et al. 1966; Dalton and Drobek 1968) and to mechanically stabilise the insulation layer. All substrates had a size of approximately 1 cm square. Both wafers and coverslips were cleaned by sonification successively in ethanol, Millipore water (Milli-Q plus 185, Millipore, Eschborn, Germany), detergent (2% Hellmanex II, no. 320.001, Hellma, Müllheim, Germany), KOH dissolved in ethanol solution and twice in Millipore water. Both silicon wafers and glass substrates were coated with laminin (GIBCO). For serum-free culture, we used neurobasal medium (GIBCO) supplemented with 0.5 mM glutamine and B27 supplement [GIBCO (Brewer et al. 1993; Brewer 1995)]. Alternatively, for serum-containing culture, cells were cultured in BME with 10% horse serum, 1 mM glutamine, supplemented with 37.5 μg/mL insulin and 2 mg/mL glucose.

Whole-cell patch-clamp recordings were obtained at room temperature (24–27 °C) under direct visual control using an upright microscope (Zeiss Axioscope) equipped with differential interference contrast optics. For cells on silicon wafers, good optical resolution was obtained with epi-illumination; trans-illumination was used for cells on glass coverslips (Fig. 1). Currents were recorded with borosilicate pipettes (outer diameter 1.5–2 μm, open tip resistance 3–5 MΩ) filled with a solution containing (mM) 110 KCl, 5 $MgCl_2$, 0.6 ethylene glycol-bis(β-aminoethyl ether)-*N*,*N*,*N*′,*N*′-tetraacetic acid, 10 *N*-2-hydoxyethylpiperazine-*N*′-2-ethanesulfonic acid and 2 Na-adenosine-5′-trisphosphate (pH set to 7.3 with KOH, 230 mosmol) and connected to an EPC-7 patch-clamp amplifier (HEKA-Electronics, Darmstadt, Germany) used without series resistance compensation ($< 20$ MΩ). The extracellular bathing solution contained (mM) 125 NaCl, 1 KCl, 1 $MgCl_2$, 20 HEPES, 10 glucose and 2 $CaCl_2$ (pH set to 7.35 with NaOH, 270 mosmol). Prior to obtaining the pipette-membrane seal, the capacitance of the recording apparatus was fully compensated. Current output was filtered at 3 kHz and digitised using a Digidata interface (Axon Instruments) controlled by an IBM compatible computer running Pclamp 6 (Axon Instruments).

### Analysis of electrophysiological data

In order to compare the development of voltage-dependent currents in neurones growing on $Si_3N_4/SiO_2$-coated Si wafers and on glass, we performed recordings on a large number ($> 30$) of cells from at least four different culture preparations for 3, 5, 7, 11 and 13 days in vitro. A total of 662 of approximately 700 recordings from different cells were of sufficient quality to be included in the present dataset, which, therefore, contains between 26 and 45 (mean 33) measurements taken at the five developmental stages in either NBM or SCM and on either glass or semiconductor substrate (i.e. 33 cells × 2 substrates × 2 media × 5 stages of development = 660 cells). As shown in Fig. 2A and E, a predetermined series of voltage pulses from a holding potential of −70 mV was applied to each cell and the resulting currents recorded. Averaged ($n = 4$) responses to small (1 mV) hyperpolarising pulses were scaled (Fig. 2B) and subtracted from all currents to substract leak and capacitive components in order to isolate the current due to voltage-dependent inward and outward conductances (Fig. 2C and F). This average was also used to estimate the access (or series) resistance, the membrane resistance and the membrane capacitance from a fit of the current with the relationship (Lindau and Neher 1988) $I(t) = (I_0 - I_\infty)\exp(-t/\tau_M) + I_\infty$, where $I(t)$ is the recorded current, $I_0$ is the instantaneous current, $I_\infty$ is the steady-state current and $\tau_M$ is the membrane time constant (Fig. 2B). The access (or series) resistance is then given by $R_A = V_{comm}/I_0$, the cell input (or whole membrane) resistance by $R_M = V_{comm}/I_\infty$ and the membrane capacitance by $C_M = \tau_M(1/R_M + 1/R_A)$, where $V_{comm}$ is the amplitude of the voltage command step.

The inward current component was abolished by inclusion of tetrodotoxin (600 nM) into the extracellular solution or by replacement of extracellular $Na^+$ with an impermeant cation such as choline (data not shown), indicating that it is carried by classical fast, voltage-dependent $Na^+$ ion channels. The outward component could be abolished by dialysis of the neurone with an internal solution containing CsCl instead of KCl and was also sensitive to extracellular TEA (data not shown), and is therefore mediated by $K^+$-selective voltage-dependent channels.

During the flow of fast and large currents, such as the voltage-dependent $Na^+$ current, the entire membrane of branching neurones like those studied here cannot be expected to be effectively clamped to the command potential. Imperfect space clamp is evident in the recording shown in Fig. 2C and F, where the voltage-

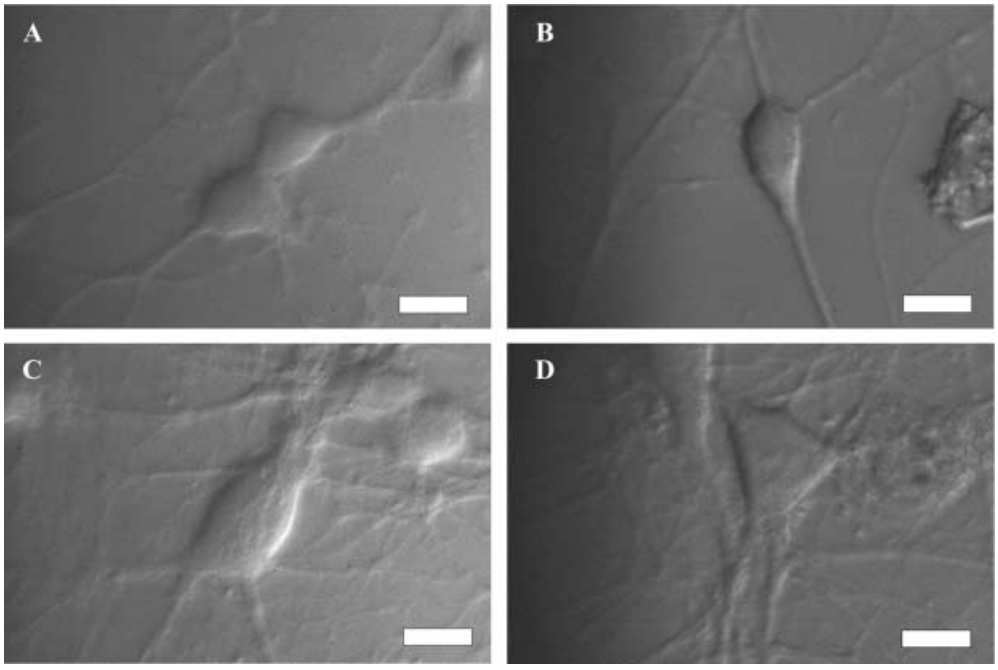


**Fig. 1A–D** Morphology of DIV 13 striatal neurones under four different culture conditions. **A** On semiconductor substrate, in neurobasal medium (NBM). **B** On glass, in NBM. **C** On semiconductor substrate, in serum-containing medium (SCM). **D** On glass, in SCM. *Scale bar*: 10 μm. Differential interference contrast images were obtained with epi-illumination on wafers (**A**, **C**) and with trans-illumination on glass (**B**, **D**). Note the greater soma size of neurones in SCM

dependent ($Na^+$) inward current appears as an all-or-nothing action current in response to threshold depolarisation. Therefore, for quantification of our results the maximal peak inward current was used independently of the size of the voltage step applied (Fig. 2C: $I_{inw,max}$). In addition, the outward current was measured both at its peak and at the end of the voltage pulse (Fig. 2C: $I_{outw,pk}$ and $I_{outw,ss}$). The outward current values thus obtained were plotted against the command potential to yield a *VI* curve each for the peak and steady-state outward currents. The outwardly rectifying part of these curves was fit with a line to obtain an estimate of the average slope conductance.

In this way, we obtained six measured values for each recorded cell: access resistance ($R_A$), membrane input resistance ($R_M$), whole cell capacitance ($C_M$), maximal inward current ($I_{inw,max}$) and maximum and steady-state slope conductance of the outward current ($g_{outw,pk}$ and $g_{outw,ss}$). Importantly, access resistance values showed no significant changes with development and were also never significantly different between groups of cells that were compared at one time point (Bonferroni/Dunn post-hoc unpaired *t*-test). Thus, differences in current or conductance density reported below cannot be ascribed to systematic differences in voltage clamp error. In addition, in order to follow the morphological development of neurones, we used digitally acquired images to estimate the size of neuronal somata as their projection area in the plane of focus (i.e. $\pi r^2$ whereby *r* is the cell radius). This value can be related to the somal membrane area by making assumptions about the somata's three-dimensional shape. Assuming a spherical geometry, the somal membrane area would be four times the projection area ($4\pi r^2$), while assuming a flat geometry with height $\rightarrow 0$, the membrane area would be given by the sum of the areas of the upper and lower sides of the cell: $2\pi r^2$. Because cells are neither spherical nor totally flat, a realistic approximation of the relationship of membrane area to projection area can be given by a factor of 3.

## Statistics

Statistical comparisons of the development of the means of the electrophysiological parameters of interest were performed using the multiple regression function of the program StatView (Abacus Concepts, Berkeley, Calif., USA). Because of the often skewed (non-Gaussian) distributions of values, comparisons between individual time points were carried out using the non-parametric Kolmogorov-Smirnov test routine of StatView. In all statistical tests, differences between distributions or mean values were considered significant at an error probability $P < 0.05$.

## Immunochemical assessment of laminin distribution

To assess qualitatively the homogeneity of laminin distribution, glass and semiconductor wafers were cleaned and coated with mouse laminin as for cell culture and incubated for 2 days with SCM in the cell culture incubator. Substrates were then fixed with 4% paraformaldehyde in phosphate-buffered saline supplemented with 0.12% sucrose and processed for immunochemical detection of laminin using a rabbit affinity-isolated antibody to laminin (L9393, Sigma, Deisenhofen, Germany). Bound antibody was visualised using a fluorescence-coupled secondary anti-rabbit IgG antibody. Fluorescence images were obtained on a confocal laser scanning microscope (Biorad).

## Contact angle measurements

In order to obtain information about the relative hydrophobicity of glass and semiconductor surfaces, we measured the contact angle of a sessile drop of water using a contact angle meter (Model G1, Krüss, Hamburg, Germany). Samples were cleaned as for cell culture and either measured (1) directly following cleaning, (2) following 1-week-long exposure to clean air or (3) following coating with laminin as for cultures.

## Surface charge measurements

Surface charges of glass and semiconductor substrates were measured using an atomic force microscope (AFM) following established methods (Raiteri et al. 1996, 1998; Zhmud et al. 1998). The AFM enables measurements of forces in the piconewton range, including the electrostatic interaction between the nanometer-sized tip of the AFM cantilever and a substrate. In solution, protons bind reversibly to both the substrate (glass or semiconductor) and the cantilever ($Si_3N_4$). Thus, by titrating their electrostatic interaction from repulsion at high pH (both substrate and cantilever charged negatively) through a region of attraction (one positive, the

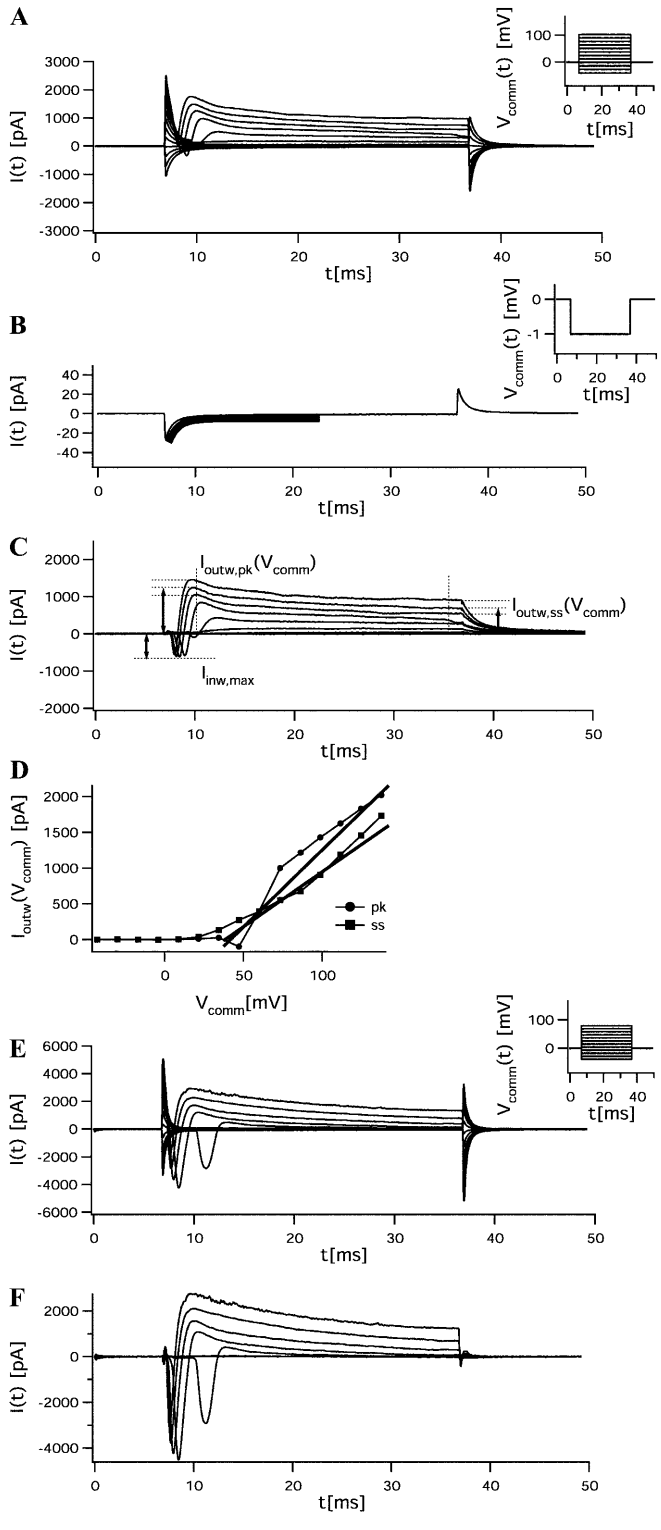


◀

**Fig. 2A–F** Analysis of current responses. **A** Current responses to a series of hyper- and depolarising voltage commands (*inset*) of a DIV 13 neurone cultured on glass in NBM. **B** Average of passive responses ($n=4$) to hyperpolarising voltage commands. The *thick line* is a monoexponential fit used to estimate the cell's passive electrical parameters. **C** Determination of maximal inward current ($I_{inw,max}$) and peak and steady-state outward current ($I_{outw,pk}$, $I_{outw,ss}$), respectively, from current responses from **A** after subtraction of an appropriately scaled version of the passive response. **D** $I_{outw,ss}$ and $I_{outw,pk}$ plotted against command potential. The *straight*, *dashed lines* are linear fits used to estimate the outwardly rectifying conductance. **E**, **F** as in **A** and **C** but from a DIV 13 neurone cultured in SCM. Note the much higher amplitude of the inward current component

other one negative) to a second region of repulsion at low pH (both charged positively), the point of zero charge of the substrate can be estimated.

Substrates were cleaned as for cell culture and placed in a low-molarity (1 mM KCl) solution to minimise shielding of surface charges by counter-ions. The pH of this solution was then set to the desired value with HCl and KOH. The low strength of the solution limited the range of pH values to between 2.5 and 10.5. Force-distance curves were recorded with a scan rate of 400 nm/s using a custom-built AFM (Oesterhelt et al. 1999) using $Si_3N_4$ cantilevers (Microlevers, Park Scientific Instruments, Sunnyvale, Calif., USA) with a spring constant of 12 mN/m. Measurements were done on two different glass and semiconductor substrates, respectively, and repeated five times at each pH value. After each pH change, 30 min were allowed for re-equilibration. For each force-distance curve, we determined the force at a distance of 15 nm from the substrate, where electrostatic interaction dominates and other forces, such as van der Waals interactions, can be disregarded.

## Results

### General observations

Neurones developing in B27-supplemented NBM, i.e. without glial cells, clearly appeared to be smaller than those growing in SCM, while morphological differences between substrates could not be detected (Fig. 1). Neurones cultured in NBM were also more prone to agglomeration in clusters and, between DIV 11 and 13, many cells cultured in NBM could be observed to have lost contact with the substrate and to deteriorate (not shown). This occurred both on semiconductor substrate and on glass. The unusually volatile behaviour of cell capacitance and inward current at these developmental stages in NBM may be related to this degenerative tendency (see below).

### Development of passive electrical parameters depends on medium but not on substrate

An overview of the development of passive electrical parameters of the neurones as estimated in this study is given in Fig. 3. Figure 3A and D show the development of cell membrane capacitance, which showed a strong increase with development. This is expected to be due to the growth of the total membrane area. Multiple regression analysis showed that cell capacitance was significantly ($P<0.005$) higher in SCM than in NBM (compare Fig. 3A and D). However, this finding was dependent on a sudden increase in the relative number of cells with very low membrane capacitance on DIV 11 (semiconductor) and DIV 13 (glass) in cells cultured in NBM. If these data points were neglected in the analysis, the difference was no longer significant ($P>0.05$). It is

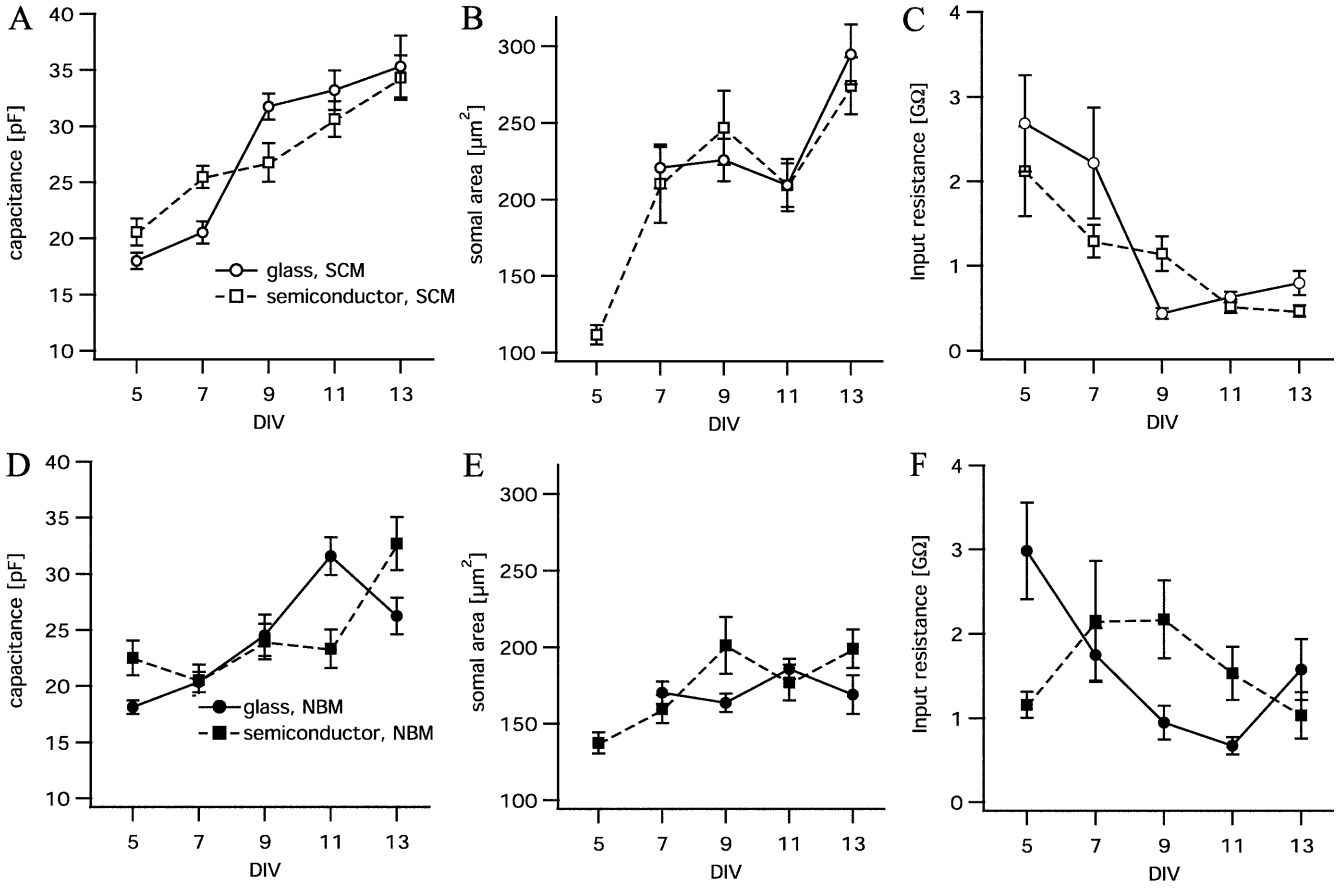


**Fig. 3A–F** Development of capacitance, somal area and input resistance under four conditions of culture. From *left to right*, mean values of (**A**, **D**) cell capacitance, (**B**, **E**) optically determined somal area (projection area) and (**C**, **F**) input resistance are given for each day in vitro (DIV). The *upper row* of graphs (**A**, **B**, **C**, *open symbols*) shows the values for neurones cultured in SCM, the *lower row* (**D**, **E**, **F**, *filled symbols*) illustrates those for cells grown in NBM. Different substrates are indicated by *circles* (glass) or *squares* (semiconductor). *Error bars* are standard errors of the mean. In **D**, note the deviations from an otherwise linear increase in capacitance on glass and on semiconductor on DIV 13 and 11, respectively. For further details, see text

possible that the low capacitance of many neurones in NBM at these stages is related to the same degenerative process that induced the loss of substrate adhesion often seen in NBM in this phase of development (see above). The fact that by DIV 13 on a semiconductor surface the mean capacitance returned to a value compatible with linear growth indicates that, indeed, the affected cells had died, and therefore did not contribute to the sample. It is clear, however, that there was no effect of substrate (glass or semiconductor) on cell capacitance ($P > 0.5$).

The increase during development of somal projection area (Fig. 3B and E) was much more pronounced in SCM than in NBM, which corroborates the impression that NBM cells were smaller in size ($P < 0.01$; cf. Fig. 1). Again, multiple regression analysis showed that substrate was without effect on soma size. While the results concerning capacitance and soma size agree in showing no effects of substrate, there is an apparent discrepancy regarding the effect of the medium: at DIV 13, for instance, the soma size in SCM cells is, on average, 60% larger than that of NBM cells, whereas the corresponding difference in cell capacitance is by only 16%. This finding might be explained if NBM cells compensated for the relative scarcity of somal membrane area by more heavily investing in neuritic membrane or if NBM cell somata assumed a more rounded shape, leading to smaller projection diameters for a given somal membrane area. Assuming the shape of neuronal somata to be approximated by a flattened sphere, we multiplied the somal projection area by a factor of 3 (see Materials and methods) to yield an approximation of somal membrane area. Dividing the total cell capacitance by this value resulted in a mean specific membrane capacitance of 4.6 ± 0.19 $\mu F/cm^2$, a value about five times higher than usually assumed for neurones. This finding indicates that, indeed, optically determined soma size is a poor gauge of true membrane area. This can be either due to the contribution of cellular processes, membrane invaginations or to variations of the cell shape.

It has been frequently observed before that both in vivo and in vitro development of neurones is associated with a monotonic decrease in neuronal resting input resistance (Fig. 3C and F), reflecting both the increase in membrane area as well as a decrease in the specific

resistance of the membrane due to the expression of leakage channels. We found a clear deviation from this pattern under one condition (Fig. 3F): cells plated in NBM on semiconductor material had significantly lower input resistance on DIV 5 than neurones plated in NBM on glass [1159 ± 154 MΩ versus 2987 ± 571 MΩ, $P < 0.005$, Kolmogorov-Smirnov (KS) test]. This value then rose to a plateau between DIV 7 and 9, where the input resistance was significantly larger than on glass ($P < 0.05$) and then took a belated decline. The other three conditions studied did not yield significant differences in the development of input resistance.

## Development of voltage-dependent properties is significantly affected by both medium and substrate

Figure 4A and B illustrate the development of voltage-dependent inward current expressed as mean peak current density from DIV 5 to 13. Two clear results may be stated:

1. First, both on glass and on semiconductor substrate, expression of the inward current was strongly dependent on the culture medium, its density being lower throughout in NBM than in SCM ($P < 0.0001$). The development of sodium current density in NBM showed a remarkable parallel with that of cell capacitance (cf. Fig. 3D), i.e. on DIV 11 (semiconductor) and 13 (glass) the values show an abrupt decline, that may, as we have said above, be linked to involution of cells due to loss of contact with the substrate. However, in this case, even after removal of these data points, the difference between media regarding the current density for inward current was very significant ($P < 0.005$).

2. Second, and somewhat surprisingly, we found a clear effect of substrate, which was, however, only seen with cells cultured in SCM. The increase in current density was clearly slower on semiconductor substrate than it was on glass, and, in fact, the current density value at DIV 13 on semiconductor substrate was only 63% of that on glass (53.5 ± 5.05 versus 85.1 ± 9.31 pA/pF). Multiple regression analysis also yielded a highly significant effect ($P < 0.001$). In order to further explore this finding, cumulative probability density plots of final (DIV 13) inward current density were constructed. They clearly show that the difference between the mean value of this parameter in semiconductor versus glass substrate in SCM at this stage is due to a near-parallel shift along the amplitude axis ($P < 0.05$, KS test).

Figure 5A and B show the development of mean steady-state outward conductance normalised to cell capacitance (i.e. a conductance density). In contrast to the voltage-dependent (Na) inward current density, there was no obvious difference on either substrate regarding development of outward conductance between neurones cultured in SCM and NBM at any except the earliest stage of development. On DIV 5, however, outward current was already well developed in SCM (Fig. 5A), and showed only little overall increase up to DIV 13. In NBM, in contrast (Fig. 5B), both on glass

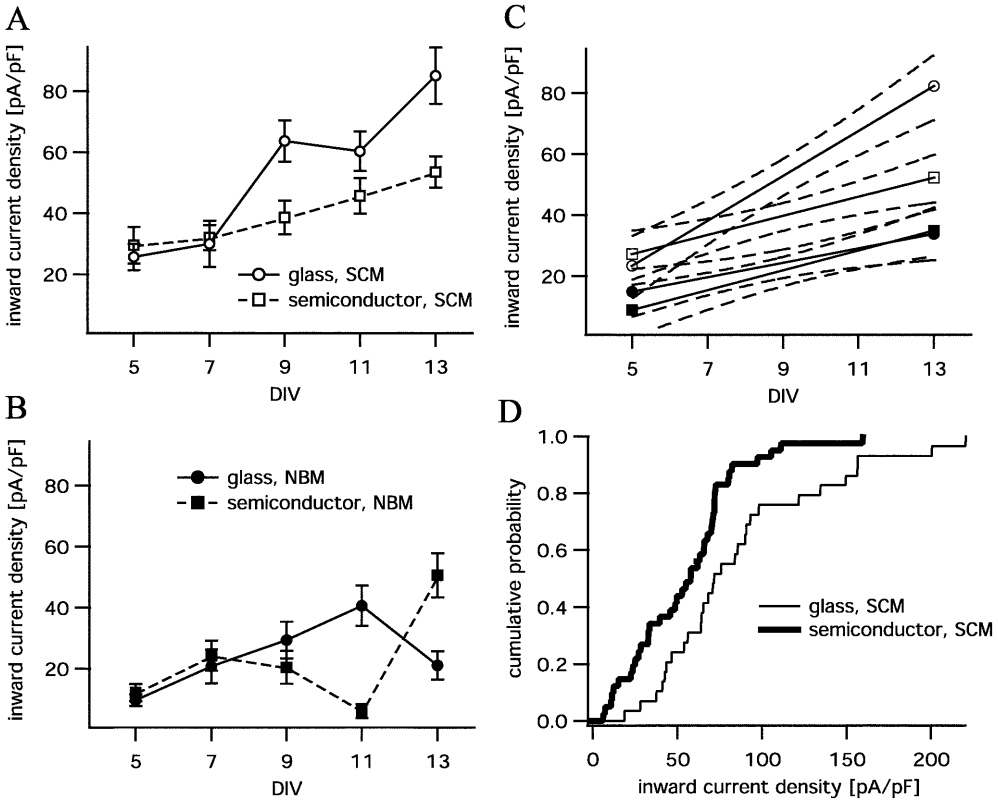


**Fig. 4A–D** Development of voltage-dependent inward current. **A** Inward current density in SCM on glass and on semiconductor. Note the lower steepness of developmental increase in current density on semiconductor (3.08 pA/pF per DIV versus 7.47 pA/pF on glass; compare panel **C**). **B** As in **A** but in NBM. Note the deviations from a linear development of current density on glass and on semiconductor on DIV 13 and 11, respectively. **C** Linear fits to the data points shown in **A** and **B**. The same symbols apply. *Dashed lines*: 95% confidence intervals. Note the absence of overlap of confidence intervals between values in NBM and SCM, indicating a significant difference throughout. For further details, see text. **D** Cumulative probability plot of current density at DIV 13 in SCM. Note the near-parallel shift towards lower amplitudes by about 24 pA/pF between glass and semiconductor

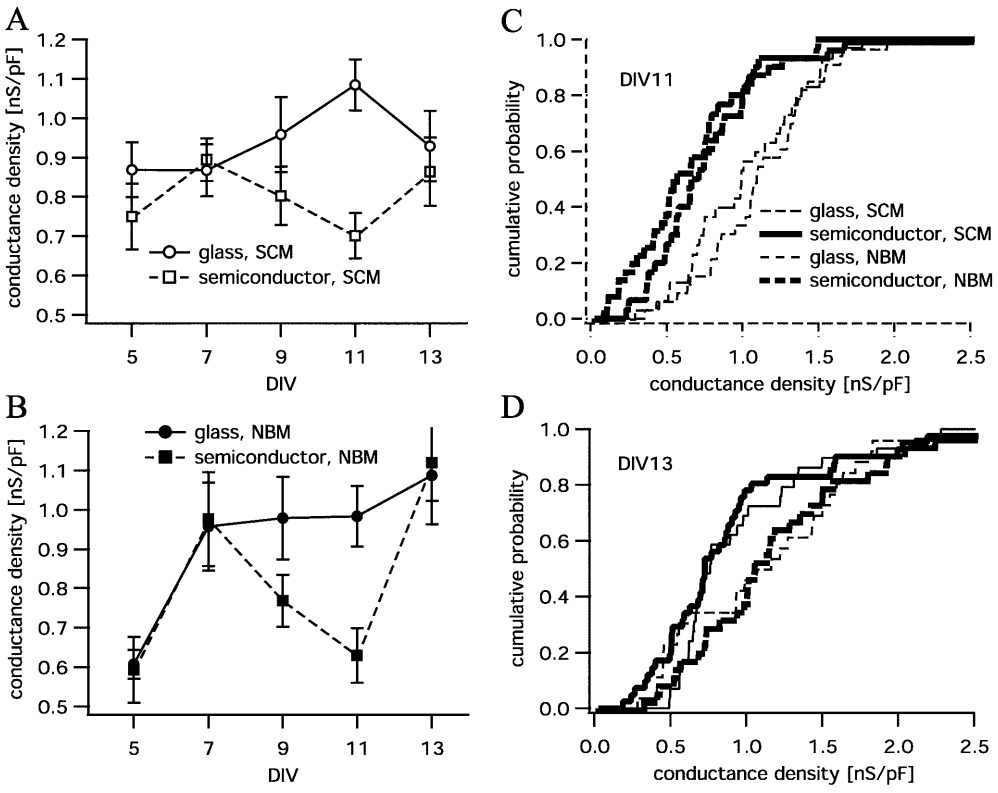


**Fig. 5A–D** Development of voltage-dependent outward current. **A**, **B** Mean outward conductance normalised to cell capacitance (i.e., conductance density) in SCM (**A**) and NBM (**B**) on glass and on semiconductor. Note the transient decline in outward current density that occurs on semiconductor only but in both types of medium around DIV11. **C**, **D** Cumulative probability plot of outward conductance density on DIV11 (**C**) and DIV13 (**D**). While the difference between semiconductor and glass is highly significant at DIV11 both in SCM and NBM, no such difference can be found at DIV13

and on semiconductor substrate we observed a pronounced increase in outward current between DIV 5 and 7. Thus, it appeared that outward current development was slightly delayed in NBM but reached the same conductance density as in SCM by DIV 7. At the same time, however, a notable difference between glass and semiconductor substrate can be appreciated in the graphs of Fig. 5A and B: in both SCM and NBM neurones, those grown on semiconductor substrate showed a pronounced dip in outward conductance density between DIV 7 and 13, so that on DIV 11 the outward current density was significantly lower ($P < 0.01$) on semiconductor surface material than on glass. No significant differences between glass and semiconductor surface persisted at DIV13 ($P > 0.1$, Fig. 5A and B). The cumulative distributions shown here also disclose a tendency for the steady-state outward conductance at DIV13 to be larger in NBM than in SCM. However, this was significant only for the cells growing on semiconductor substrate.

It should be noted as an important fact that, unlike in the case of the transient apparent loss of inward current in NBM that was described above, there was no evidence for a link between the transient decrease of outward current on semiconductor surface and loss of cell adhesion. The temporary reduction in mean inward current on DIV 11 and 13 was seen on glass and semiconductor substrate but only in NBM medium (Fig. 4B), and furthermore conformed with similar movements of mean cell capacitance (cf. Fig. 3D), while outward current on DIV 11 was significantly reduced *both* in NBM and SCM but occurred *only* on semiconductor substrate.

## Contact angle measurements show significant differences in hydrophobicity between uncoated, but not laminin-coated, glass and semiconductor surfaces

Immediately following cleaning, uncoated glass surfaces showed a contact angle with water of $7 \pm 0.5°$, while semiconductor surfaces had contact angles of $13 \pm 6°$. When glass and semiconductor surfaces were exposed to air for 1 week, contact angles increased to $21 \pm 2°$ and $30 \pm 6°$, respectively. Both these differences are highly significant ($P < 0.0001$, unpaired, one-tailed *t*-test) and show that semiconductor surfaces are more hydrophobic than coverslip glass. After coating with laminin, however, contact angles were strongly increased and became equal for both substrates ($57 \pm 4°$ and $57 \pm 5°$, respectively).

## Distribution of laminin is homogeneous on both substrates

The distribution of laminin on glass and semiconductor substrate was assessed using immunochemical fluorescence staining and confocal laser scanning microscopy on four samples of each variety (see Materials and methods). Laminin fluorescence appeared homogeneous

with sparse clusters of higher intensity on both types of the substrate. In particular, areas lacking laminin fluorescence were never observed either on glass or on semiconductor surfaces (data not shown), indicating that laminin deposition was not affected by the substrates.

## Atomic force microscopy shows differences in surface charge between glass and semiconductor substrates

Surface charge is an important factor in cell adhesion (Torimitsu and Kawana 1990; Soekarno et al. 1993; Healy et al. 1994; Qiu et al. 1998; Rajnicek et al. 1998; Nicolau et al. 1999; Schottelndreier et al. 1999). We therefore intended to investigate possible differences in the surface charge between glass and semiconductor surfaces in solution using force-distance curve measurements with the AFM. Two typical force-distance curves are shown in Fig. 6A. With distances $>50$ nm there is no observable interaction between the cantilever tip and the substrate; thus no force is measured. While approaching the cantilever to the substrate further, at pH 10.18 they repel each other. This can be explained by surface charges of equal polarity on substrate and cantilever, resulting in a negative force. At pH 2.65, attraction results because substrate and cantilever are oppositely charged. The interaction of cantilever and substrate can be seen to decrease exponentially with distance $d$, with a decay constant given by the Debye length. At $d=0$ the cantilever touches the substrate, which it cannot penetrate (hard core repulsion). As a measure of the interaction, we measured the force acting between cantilever and substrate at a distance of 15 nm [$F$(15 nm)], where electrostatic forces dominate and van der Waals forces or other types of interaction can be neglected. We also calculated the force at $d=8$ nm, which gave similar results. In Fig. 6B the relationship between pH and $F$(15 nm) is shown for two glass

**Fig. 6A, B** Surface charge measurements using the scanning force microscope. **A** Typical force-distance curves recorded on semiconductor substrate. Positive forces $F$ indicate attraction. The *black curve* was recorded at pH 2.65, the *grey curve* at pH 10.18. Note the exponential increase of attractive (pH 2.65) and repellant (pH 10.18) force with distance $<30$ nm. The *vertical dashed line* indicates the distance of the cantilever ($d=15$ nm) at which force measurements [$F$(15 nm)] were taken. The force curves are not continuous until $d=0$ because the cantilever snaps into contact with the substrate at $d>0$ owing to short-range interactions, such as van der Waals attraction. **B** Mean values ± standard deviation obtained from five force-distance curves taken on two different glass (*grey curves*) and semiconductor samples (*black curves*). The symbols (×) and (○) indicate the different samples, respectively. The *horizontal dotted line* indicates zero force, the *vertical dashed line* is at pH 7. Note that the curves for semiconductor substrate cross the zero force line twice, between pH 6–7 and between pH 3–4, whereas the curves for glass substrate appear to cross only once, below pH 4

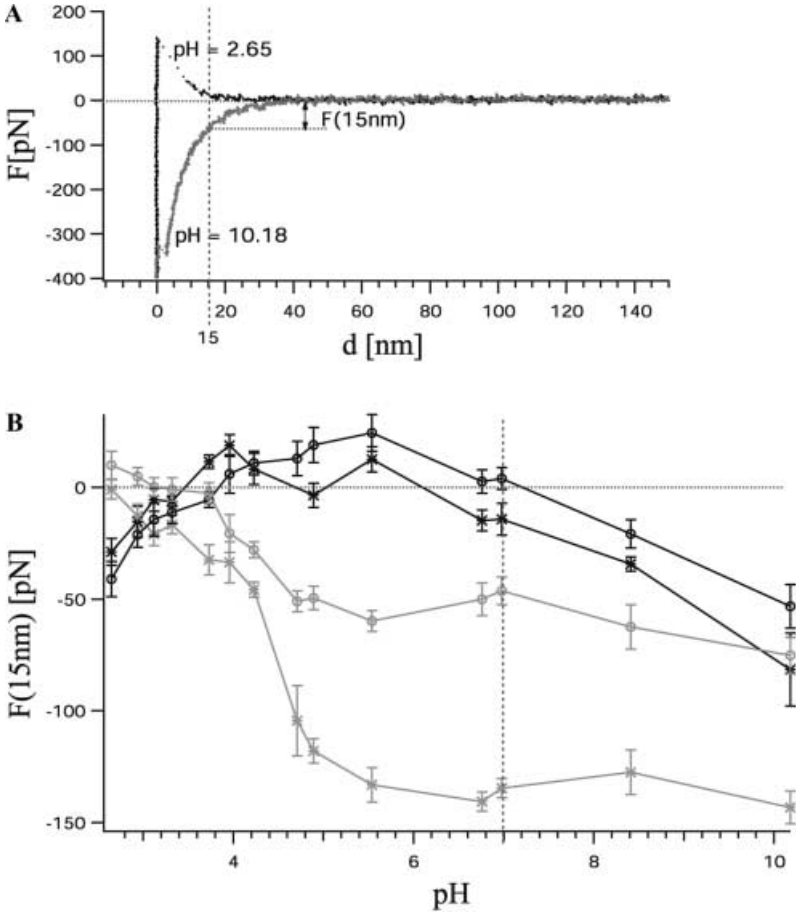

substrates and two semiconductor substrates. Semiconductor substrates show repulsion both for pH values $>6$–7 and $<3.5$–4 and attraction in-between those values. In contrast, glass substrates repel the cantilever at all pH values $>3$–4, while we cannot exclude attraction at levels much below 3. At neutral pH, the semiconductor substrates do not strongly interact with the cantilever, whereas there is clear repulsion between glass substrate and cantilever. This result points towards important differences in surface charge of the two types of substrate.

## Discussion

The main findings of the present study are the following:

1. Rat striatal neurones cultured in NBM show a selective reduction in the density of voltage-dependent inward, but not outward, conductances with respect to those cultured in SCM. This effect was associated with a smaller somal size of NBM-fed compared to SCM-fed neurones.
2. SCM-grown neurones cultured on glass showed a significantly better development of voltage-dependent inward current than those growing on the semiconductor surface. No such effect of substrate on inward current expression could be demonstrated for cells growing on NMB.
3. On semiconductor surface substrate only, a transient decline was found in the voltage-dependent outward conductance around DIV 11 in both NBM- and SCM-fed neurones. This effect was not detected on glass.
4. Semiconductor substrate and glass had significantly different pH-dependent attraction-repulsion behaviour in AFM measurements, suggesting differences in surface charge.

### Effects of neurobasal medium versus serum-containing medium

Cells cultured in NBM had significantly smaller soma sizes than cells grown in SCM. The fact that, in contrast, they did not have lower capacitances than SCM cells may be taken as evidence that NBM cells have more effusive neuritic branching than do cells in SCM.

To our knowledge, since the introduction of NBM supplemented with B27 four years ago, no published account of the development of voltage-dependent conductances under these serum/glia-free conditions has been given. Our findings suggest a significant and selective impairment of the development of voltage-dependent inward but not outward current densities with respect to conventional serum-supplemented medium. In principle, either absence of a direct effect of serum-derived trophic factors or lack of growth factors of glial origin could account for this developmental alteration. Regardless, culture in B27-supplemented NBM does appear to have clear disadvantages against SCM culture. However, glia-free cell culture is desirable or, in fact, necessary for the construction of neurone-semiconductor interfaces because direct electrical coupling between neurone and semiconductor would be made impossible by an interposed glial layer. It will be useful, therefore, to test other, more complex, formulations for glial-free neuronal culture media (Weiss et al. 1986; Sebben et al. 1990; Kowalski et al. 1995).

### Effects of semiconductor surface versus glass substrate

Of the two effects of semiconductor substrate that were observed in this study, an impaired development of inward current with respect to glass substrate was only observed under SCM conditions, i.e. in neuro-glial cocultures. This might indicate that the effect was due to an interference of the substrate with glial function, reducing a trophic influence mediated by glial cells on $Na^+$ channel development (cf. Kaplan et al. 1997). Because no glial cells are present in NBM-fed cultures, such effects would not be expected to be seen there.

A most unusual finding in this study is the transient reduction or "dip" in outward current density that was found on semiconductor material only, centred around DIV11 both in SCM and NBM. Such an effect might be explained if, during development, there was a shift in the expression of different types of channel protein subunit, which under normal conditions were arranged such that a "smooth take-over" is possible and no decrease in the density of functional channels occurs at the transition. If, however, the expression of a second subunit was for some reason delayed, a gap might become visible.

### Is semiconductor substrate biologically equivalent to glass?

An obvious difference between the silicon wafers and the glass coverslips used here lies in fact that the latter are pure insulators, whereas in the case of the wafers the insulating coat of $Si_3N_4/SiO_2$ is $<100$ nm thick and covers a 1-mm-thick, doped semiconductor layer. Any influence of this fact on cellular development, however, is highly speculative.

In general, cell development may be influenced by five substrate properties which could be different between glass and $Si_3N_4$ surfaces: (1) chemically reactive groups, (2) charge, (3) hydrophobicity, (4) roughness and (5) the amount of adsorbed protein, with the last parameter dependent on the preceding four. In addition, (1)–(5) are not easy to discriminate as they may influence each other (Singhvi et al. 1994).

*Chemical composition*

Chemically, glass and semiconductor substrates used in this study are different chiefly because coverslip glass contains about 40% of metal oxides other than $SiO_2$ (see Materials and methods). However, all the constituents of both the coverslip glass and the wafers are highly inert and, therefore, chemical reactions with the cells or with the underlying laminin are unlikely.

*Surface charge*

Surface charge is well known to influence cell adhesion (Healy et al. 1994). There is evidence that cells preferentially adhere to and grow on positively charged surfaces (Torimitsu and Kawana 1990; Soekarno et al. 1993; Healy et al. 1994; Qiu et al. 1998; Rajnicek et al. 1998; Nicolau et al. 1999; Schottelndreier et al. 1999). This preference appears logical, given the fact that the membrane glycocalix carries a net negative charge. Coating of glass substrates with basic amino acid polymers such as poly-lysine and poly-ornithine was introduced in the first place to compensate for the negative surface charge of glass (Higgins and Banker 1998). Laminin, on the other hand, is a complex protein, which promotes cell adhesion and development by specific binding to cellular receptors rather than simple masking of surface charges (Kleinman et al. 1990; Mercurio and Shaw 1991; Mecham 1991a, 1991b; Tanzer et al. 1993; Tryggvason 1993; Engvall and Wewer 1996; McKerracher et al. 1996). Laminin itself is known to bind preferentially to negatively charged surfaces (Clegg et al. 1988; Poschl et al. 1996; Elias et al. 1999). This might be due to the lysine-rich, positively charged domain of the protein (Stetefeld et al. 1996). The other side of the laminin macromolecule is negatively charged; thus, laminin-coated surfaces are likely to carry net negative charge (Rajnicek et al. 1998).

In contact with electrolytes, metal oxides and metal nitrides such as $SiO_2$ and $Si_3N_4$ are able to accept or release protons, depending on the pH of the solution. For instance, $SiO_2$ surfaces express silanol (Si-OH) sites which are positively charged ($Si\text{-}OH_2^+$) at very low pH and negatively charged ($Si\text{-}O^-$) at high pH. $Si_3N_4$ surfaces express primary amine ($Si\text{-}NH_2$, silamin) sites as well as silanol sites (Harame et al. 1987; Bousse and Mostarshed 1991). Thus, at low pH, the surfaces of these substrates are charged positively, while they carry net negative charge at high pH. The pH value where the net charge of the surface is zero is called $pH_{pzc}$ (pcz: point of zero charge). In our measurements using the AFM, the $pH_{pzc}$ is indicated by a point of reversal of the direction of interaction from attraction to repulsion. At this pH, thus, there is no electrostatic force between substrate and cantilever. However, such reversal of direction can occur either because the substrate or the cantilever (which consists of $Si_3N_4$ and will equally react with protons) carries no net charge. In the case of the semiconductor substrate (cf. Fig. 6B), there are two values of pH where the force of interaction approaches zero: one lies between pH 6 and 7 and the other between pH 3.5 and 4. Raiteri et al. (1998) have found $pH_{pcz} = 4.5$ for the same AFM cantilever as used in this study and $pH_{pcz} = 5.6$–$6.4$ for semiconductor surfaces of light-addressable photometric sensors (LAPS) and ion-sensitive field-effect transistors (ISFET), which are similar in composition to the semiconductor surfaces used here. Thus, it is likely that, in our measurements, the $pH_{pzc}$ between 6 and 7 represents the point of zero charge of the semiconductor-substrate while that between 3.5 and 4 corresponds to electrical neutrality of the cantilever. Also in agreement with this interpretation is the fact that, in our experiments with glass substrate, force reversal also occurred at pH 3 and 4. We did not observe a second crossing of the zero-force line with glass substrate, suggesting that the $pH_{pzc}$ of the glass surface is either the same as that for the cantilever or lies well below that value. Raiteri et al. quote a value of $pH_{pcz} = 3.5$ for glass, which would be in line with our findings. At $pH = 7.4$, the AFM cantilever is negatively charged, because its $pH_{pzc} \ll 7.4$. At this pH, also, glass would be maximally negatively charged (i.e. all silanol sites would have released their protons). Thus, in this situation, the force of interaction [$F$(15 nm)] would approach saturation, because both glass and cantilever have shed all their protons, carry saturated negative charge and repel each other. In contrast, at $pH = 7.4$ the semiconductor substrate is nearly without charge or carries a much smaller negative charge. Only at $pH > 7.4$ would the semiconductor surface release more protons, increasing its negative charge. Saturation would only occur with $pH \gg 6$–$7$.

The glass used in our study, as well as in cell culture applications in general, is not pure $SiO_2$ (i.e. quartz glass) but contains other metal oxides. $TiO_2$ and $Al_2O_3$ (present at 4% and 6.4%, respectively) have a higher $pH_{pzc}$ than $SiO_2$, i.e. they are more negatively charged than $SiO_2$ at a given pH (Smit and Holten 1980; Jayaweera and Hettiarachchi 1993; Mathur and Moudgil 1997; Mustafa et al. 1998). The $pH_{pzc}$ of the glass used here would then be expected to be higher than that of pure $SiO_2$. The fact that our measurements agree well with published values of $pH_{pzc}$ for $SiO_2$, however, suggests that these additional metal oxides do not greatly contribute to the expression of surface charges.

In summary, then, our measurements of surface charge, in accordance with those of Raiteri et al., clearly show that, at pH 7.4, the semiconductor surface used here will be almost without net surface charge, whereas the glass substrate is clearly negatively charged. Thus, there is a clear difference in surface charge between glass and semiconductor substrate. This finding contrasts with measurements by Bousse and Mostarshed (1991), who concluded that $SiO_2$ and $Si_3N_4$ had very similar surface charge, as well as with our own previous interpretation (Parak et al. 1999).

However, it should be stressed that $pH_{pzc}$ may vary strongly according to details of the preparation. Re-

cently, Raiteri et al. (1998) have found variations in the relative primary amine content between 4 and 12% for differently manufactured devices, whereas Bousse and Mostarshed (1991) claim that, for $Si_3N_4$, the surface in contact with an electrolyte comprises less than 2% of amine sites and more than 98% of silanol sites. The higher the percentage of amine sites, the higher the $pH_{pzc}$ and, therefore, the less negatively charged the surface at pH 7.4 will be. In addition, it has been shown that, although the surface of $Si_3N_4$ in electrolyte solution consists mainly of silanol sites, owing to the instability of this oxygen-rich layer in solution, more and more amine sites are exposed over time (Mikolajick et al. 1999), a process that continued over approximately 12 days in a 0.5 mM KCl solution. As mentioned above, this is equivalent to a reduction in negative surface charge. Thus, our finding that, at pH 7.4, glass is negatively charged whereas semiconductor surface is practically neutral is valid only for the glass used here and the semiconductor substrate as prepared by us.

We can conclude with certainty from our measurements that neither glass nor the semiconductor substrate were positively charged. The fact that, in SCM-cultured neurones, voltage-dependent inward current developed faster on glass, which was in fact, more negatively charged, cannot be accounted for by the preference of neurones or glial cells for positively charged surfaces. However, it is possible that the differences in surface charge of the two substrates affected the adsorption or orientation of extracellular proteins, such as laminin, as will be discussed below.

*Hydrophobicity*

Hydrophobicity may also play a role in cell adhesion (Horbert et al. 1988) and it is chemically plausible that $Si_3N_4$ is less hydrophilic than glass. Hydrophobicity can be measured as the contact angle between a drop of water and the substrate, where small contact angles ($\rightarrow 0°$) indicate wetting of a hydrophilic surface whereas large angles ($\rightarrow 180°$) indicate hydrophobic interaction (Israelachvili 1992). Neurones prefer hydrophilic surfaces (Nicolau et al. 1999) and highly hydrophobic substrates like Teflon (O'Brien 1996) prevent neuronal growth (Makohliso et al. 1998). Adhesion of neurones is also prevented by coating of substrates with hydrophobic alkane chains (Kleinfeld et al. 1988). Plastic petri dishes, a standard substrate in cell culturing, have contact angles well above those for glass [glass: 14° (O'Brien 1967); polystyrene dishes: 66° (Arshady 1993) or 86° (Craig et al. 1960)]. The contact angles with water on glass and semiconductor substrates used here were significantly different before laminin coating, suggesting that the latter is slightly less hydrophilic than the former. However, this difference was small compared to the difference between glass and plastic culture dishes. Furthermore, the difference disappeared after coating with laminin, where both showed contact angles similar to untreated plastic petri dishes. Thus, differences in hydrophobicity are unlikely to have contributed to the biological effects of the substrates.

*Roughness*

The effect of roughness on cellular adhesion and differentiation depends on cell type (for a review, see Singhvi et al. 1994). Structures with dimensions in the range of cell size ($> 10$ μm) may influence cell growth. Thus, cells may be made to extend in a preferred direction along trenches in the substrate (Hirono et al. 1988; Clark et al. 1990). More importantly for this study, roughness on a smaller (sub-micron) scale is known to affect cells in a cell-type specific manner, e.g. fibroblasts prefer smooth surfaces (Singhvi et al. 1994) whereas macrophages and bone cells grow preferentially on rough substrates (Rich and Harris 1981; Degasne et al. 1999). For some other cells, substrate roughness does not seem to play a role for growth (Richards 1996).

Previously, using AFM, we imaged surfaces of glass and silicon-based semiconductor substrates (Parak et al. 1999) and found no significant difference in roughness defined as the integral of deviations from the mean height in the principal plane of 100 $\mu m^2$ samples.

*Protein adsorption*

Coating of culture substrates is essential for cell adhesion. For instance, the distance between cells and substrate on $SiO_2$-based surfaces is determined by the nature of the coating material and has been shown to depend more on the kind of coating used (e.g. fibronectin, laminin, poly-lysine) than on the cell type (Braun and Fromherz 1997). In the case of SCM cultures, proteins from serum adsorb on the surface of the substrate and may, in addition to laminin adsorption, contribute to masking the properties of the naked substrate (Domke et al. 2000). This reasoning would predict that greater effects of substrate would be observed in serum-free than in serum-containing media. However, in the present study, substrate-dependent effects were only observed in SCM cultures, suggesting that either the presence of serum or of glial cells (for which serum is permissive) unmasks rather than masks the substrate effects.

The amount of adsorbed protein also critically depends on surface properties. For instance, certain alkane-thiols are able to augment protein adsorption through hydrophobic interaction (Mrksich et al. 1997). Laminin, which we used to coat our substrates, also adheres better to hydrophobic substrates than to glass (Clark et al. 1993; Matsuzawa et al. 1997). Because laminin carries a positively charged moiety, it is conceivable that the less negative charge of the semiconductor might result in adsorption of less laminin. However, our fluorescence measurements using a laminin antibody did not provide evidence in this direction.

Alternatively, the lack of negative charge might influence the orientation of laminin on the semiconductor surface, which might result in a less efficient binding interaction with its cellular receptors, thus reducing its trophic effects. It is known that not only the amount of protein adsorbed but also its conformation or orientation is important for its biological effects (Chinn et al. 1991; Healy et al. 1994). It is thus conceivable that the biological function of laminin may have been compromised on semiconductor surfaces because of their smaller negative charge, preventing the molecule from attaining the orientation or conformation necessary for interaction with its receptors.

It should be noted that this discussion so far only applies to static systems in which the surface remains unchanged. However, a cell may well change its substrate during development (Biran et al. 1999; Chiquet 1999).

In summary, we here report, firstly, that glia-free culture in NBM compromises the ability of striatal neurones to express voltage-dependent ($Na^+$) inward current but not ($K^+$) outward current. This finding is in line with the assumption that the expression of $Na^+$ channels is under the control of a number of growth factors, some of which may be liberated by glial cells. We have not been able to resolve an effect of serum-free culture on outward currents that might be expected from work on hippocampal neurones based on a comparison of cells in the same culture growing on-glia or off-glia (Wu and Barish 1994).

Secondly, we have observed two significant effects of semiconductor substrate on the development of voltage-dependent currents in rat striatal neurones: a reduction in ($Na^+$) inward current that appeared dependent on the presence of glial cells (i.e. only occurred in SCM) and a transient loss of ($K^+$) outward current that was independent of the medium. Using surface charge measurements with the AFM, we have provided clear evidence that the semiconductor substrate was strongly less negatively charged than the glass surface, while other parameters, such as roughness and hydrophobicity, did not appear to be different enough to produce biological effects. Fluorescent antibody detection of laminin did not provide evidence for differences in the amount and homogeneity of distribution on a micrometre scale of laminin on glass and semiconductor substrate. However, given the polar organisation of the laminin molecule, it is possible that the reduced surface negativity of the semiconductor substrate results in a less oriented deposition of laminin, which may render less effective its interactions with neurones and/or glial cells that are likely to underlie its trophic effects. Following this hypothesis, the slowing of inward current development on semiconductor substrate that was only observed in SCM neurones (i.e. neuroglial cocultures) would then be due to a relative lack of a trophic factor that might be produced by glial cells in a manner that depends on specific interactions with laminin. The transient loss of outward current on semiconductor substrate, in contrast, that was observed irrespective of culture medium, might be due to an impairment of direct effects of laminin on neurones.

It should be stressed that, while this hypothesis must remain preliminary in the absence of direct information on the relationship between laminin orientation and its trophic actions, it provides a plausible link between decreased surface negativity and effects of neuronal development. Also, our findings cannot be generalised to all neuronal cell types and culture conditions. We conclude nevertheless that, for the development of long-term neurone-semiconductor hybrids, further detailed studies of neuronal development under various culture conditions optimised for close contact is warranted. In particular, our findings show that the equivalence for biological purposes of glass and the surface of silicon semiconductor devices, that we previously concluded from experiments with cardiomyocytes (Parak et al. 1999), cannot be taken for granted in the case of neurones. In particular, in addition to improvement of cell culture media, an appropriate modification of surfaces must also be considered to enhance the development of neuronal electrogenesis in neurone-semiconductor hybrids.

**Acknowledgements** We thank Prof. Gerrit ten Bruggencate for continuing support and encouragement, Luise Kargl and Anke Grünewald for excellent technical assistance, Dr. Eva Rumpel for help with cell preparation and Dr. Andreas Offenhäusser and Andreas Ostermann for helpful discussions. This work was supported in part by the Bundesministerium für Bildung und Forschung (BMBF grant no. 0310845A, W.J.P., M.G., H.E.G.).

## References

Arshady R (1993) Microspheres for biomedical applications: preparation of reactive and labelled microspheres. Biomaterials 14: 5–15

Bergveld P (1970) Development of an ion-sensitive solid-state device for neurophysiological measurements. IEEE Trans Biomed Eng 17: 70–71

Biran R, Noble MD, Tresco PA (1999) Characterization of cortical astrocytes on materials of differing surface chemistry. J Biomed Mater Res 46: 150–159

Bousse L, Mostarshed S (1991) The zeta potential of silicon nitride thin films. J Electroanal Chem 302: 269–274

Braun D, Fromherz P (1997) Fluorescence interference-contrast microscopy of cell adhesion on oxidized silicon. Appl Phys A 65: 341–348

Brewer GJ (1995) Serum-free B27/neurobasal medium supports differentiated growth of neurons from the striatum, substantia nigra, septum, cerebral cortex, cerebellum, and dentate gyrus. J Neurosci Res 42: 674–83

Brewer GJ, Torricelli JR, Evege EK, Price PJ (1993) Optimized survival of hippocampal neurons in B27-supplemented neurobasal: a new serum-free medium combination. J Neurosci Res 35: 567–76

Chinn JA, Horbett TA, Ratner BD (1991) Baboon fibrinogen adsorption and platelet adhesion to polymeric materials. Thromb Haemost 65: 608–617

Chiquet M (1999) Regulation of extracellular matrix gene expression by mechanical stress. Matrix Biol 18: 417–426

Clark PC, Dow JA, Wilkinson CD (1990) Topographical control of cell behaviour. II. Multiple grooved substrata. Development 108: 635–644

Clark P, Britland S, Connolly P (1993) Growth cone guidance and neuron morphology on micropatterned laminin. J Cell Sci 105: 203–212

Clegg DO, Helder JC, Hann BC, Hall DE, Reichardt LF (1988) Amino acid sequence and distribution of mRNA encoding a major skeletal muscle laminin binding protein: an extracellular matrix-associated protein with an unusual COOH-terminal polyaspartate domain. J Cell Biol 107: 699–705

Craig RG, Berry GC, Peyton FA (1960) Wetting of poly(methyl methyacrylate) and polystyrene by water and saliva. J Phys Chem 64: 541–543

Dalton JV, Drobek J (1968) Structure and sodium migration in silicon nitride films. J Electrochem Soc Solid State Sci 115: 865–868

Degasne I, Basle MF, Demais V, Hure G, Lesourd M, Grolleau B, Mercier L, Chappard D (1999) Effects of roughness, fibronectin and vitronectin on attachment, spreading, and proliferation of human osteoblast-like cells (Saos-2) on titanium surfaces. Calif Tissue Int 64: 499–507

Domke J, Dannöhl S, Parak WJ, Müller O, Aicher WK, Radmacher M (2000) Substrate dependent differences in morphology and elasticity of living osteoblasts investigated by atomic force microscopy. Colloids Surf B (in press)

Elias MC, Veiga SS, Gremski W, Porcionatto MA, Nader HB, Brentani RR (1999) Presence of a laminin-binding chondroitin sulfate proteoglycan at the cell surface of a human melanoma cell Mel-85. Mol Cell Biochem 197: 39–48

Engvall E, Wewer UM (1996) Domains of laminin. J Cell Biochem 61: 493–501

Evans MS, Collings MA, Brewer GJ (1998) Electrophysiology of embryonic, adult and aged rat hippocampal neurons in serum-free culture. J Neurosci Methods 79: 37–46

Gottmann K, Dietzel ID, Lux HD, Huck S, Rohrer H (1988) Development of inward currents in chick sensory and autonomic neuronal precursor cells in culture. J Neurosci 8: 3722–3732

Gross GW, Rieske E, Kreutzberg GW, Meyer A (1977) A new fixed-array multi-microelectrode system designed for long-term monitoring of extracellular single unit neuronal activity in vitro. Neurosci Lett 6: 101–105

Gross GW, Harsch A, Rhoades BK, Göpel W (1997) Odor, drug and toxin analysis with neuronal networks in vitro: extracellular array recording of network responses. Biosens Bioelectron 12: 373–393

Harame DL, Bousse LJ, Shott JD, Meindl JD (1987) Ion-sensing devices with silicon nitride and borosilicate glass insulators. IEEE Trans Electron Devices 34: 1700–1707

Healy KE, Lom B, Hockberger PE (1994) Spatial distribution of mammalian cells dictated by material surface chemistry. Biotechnol Bioeng 43: 792–800

Higgins D, Banker G (1998) Primary dissociated cell cultures. In: Banker G, Goslin K (eds) Culturing nerve cells. MIT Press, Cambridge, Mass., pp 37–78

Hirono T, Torimitsu K, Kawana A, Fukuda J (1988) Recognition of artificial microstructures by sensory nerve fibers in culture. Brain Res 446: 189–194

Horbert TA, Waldburger JJ, Ratner BD, Hoffman AS (1988) Cell adhesion to a series of hydrophilic-hydrophobic copolymers studied with a spinning disc apparatus. J Biomed Mater Res 22: 383–404

Israelachvili JN (1992) Intermolecular and surface forces, 2nd edn. Academic Press, London

Jayaweera P, Hettiarachchi S (1993) Determination of zeta potential and pH of zero charge of oxides at high temperature. Rev Sci Instrum 64: 524–528

Kaplan MR, Meyer Franke A, Lambert S, Bennett V, Duncan ID, Levinson SR, Barres BA (1997) Induction of sodium channel clustering by oligodendrocytes. Nature 386: 724–728

Kleinfeld D, Kahler KH, Hockberger PE (1988) Controlled outgrowth of dissociated neurons on patterned substrates. J Neurosci 8: 4098–4120

Kleinman HK, Sephel GC, Tashiro K, Weeks BS, Burrous BA, Adler SH, Yamada Y, Martin GR (1990) Laminin in neuronal development. Ann NY Acad Sci 580: 302–310

Kowalski C, Crest M, Vuillet J, Pin T, Gola M, Nieoullon A (1995) Emergence of a synaptic neuronal network within primary striatal cultures seeded in serum-free medium. Neuroscience 64: 979–993

Lamoureux P, Zheng J, Buxbaum RE, Heidemann SR (1992) A cytomechanical investigation of neurite growth on different culture surfaces. J Cell Biol 118: 655–661

Lindau M, Neher E (1988) Patch-clamp techniques for time-resolved capacitance measurements in single cells. Eur J Physiol Plügers Archiv 411: 137–146

MacDermott AB, Westbrook GL (1986) Early development of voltage-dependent sodium currents in cultured mouse spinal cord neurons. Dev Biol 113: 317–326

Makohliso SA, Giovangrandi L, Léonard D, Mathieu HJ, Ilegems M, Aebischer P (1998) Application of Teflon-AF thin films for bio-patterning of neural cell adhesion. Biosens Bioelectron 13: 1227–1235

Mathur S, Moudgil BM (1997) Adsorption mechanism(s) of poly(ethylene oxide) on oxide surfaces. J Colloid Interface Sci 196: 92–98

Matsuzawa M, Umemura K, Knoll W, Beyer D, Sugioka K (1997) Micropatterning of neurons using organic substrates in culture. Thin Solid Films 305: 74–79

McKerracher L, Chamoux M, Arregui CO (1996) Role of laminin and integrin interactions in growth cone guidance. Mol Neurobiol 12: 95–116

Mecham RP (1991a) Laminin receptors. Annu Rev Cell Biol 7: 71–91

Mecham RP (1991b) Receptors for laminin on mammalian cells. FASEB J 5: 2538–2546

Mercurio AM, Shaw LM (1991) Laminin binding proteins. Bioessays 13: 469–473

Mikolajick T, Kühnhold R, Schnupp R, Ryssel H (1999) The influence of surface oxidation on the pH-sensing properties of silicon nitride. Sens Actuators B 57: 450–455

Mrksich M, Dike LE, Tien J, Ingber DE, Whitesides GM (1997) Using microcontact printing to pattern the attachment of mammalian cells to self-assembled monolayers of alkanethiolates on transparent films of gold and silver. Exp Cell Res 235: 305–313

Mustafa S, Dilara B, Neelofer Z, Naeem A, Tasleem S (1998) Temperature effect on the surface charge properties of gamma-Al2O3. J Colloid Interface Sci 204: 284–293

Nicolau DV, Taguchi T, Taniguchi H, Tanigawa H, Yoshikawa S (1999) Patterning neuronal and glia cells on light-assisted functionalised photoresists. Biosens Bioelectron 14: 317–325

O'Brien WJ (1967) Capillary penetration of liquids between dissimilar solids. Doctoral Dissertation, University of Michigan, Ann Arbor

O'Brien WJ (1996) Biomaterials properties database: http://www.lib.umich.edu/libhome/dentistry.lib/dental_tables/contangle.html

Oesterhelt F, Rief M, Gaub HE (1999) Single molecule force spectroscopy by AFM indicates helical structure of poly(ethylene-glycol) in water. New J Phys 1: 6.1–6.11

Offenhäusser A, Rühe J (1995) Neuronal cells cultured on modified microelectronic device surfaces. J Vaccum Sci Technol A 13: 2606–2612

Offenhäusser A, Sproessler C, Matsuzawa M, Knoll W (1997) Electrophysiological development of embryonic hippocampal neurons from the rat grown on synthetic thin films. Neurosci Lett 223: 9–12

Parak WJ, Domke J, George M, Kardinal A, Radmacher M, Gaub HE, deRoos ADG, Theuvenet APR, Wiegand G, Sackmann E, Behrends JC (1999) Electrically excitable NRK fibroblasts: a new model system for cell-semiconductor hybrids. Biophys J 76: 1659–1667

Poschl E, Mayer U, Stetefeld J, Baumgartner R, Holak TA, Huber R, Timpl R (1996) Site-directed mutagenesis and structural

interpretation of the nidogen binding site of the laminin gamma1 chain. EMBO J 15: 5154–5159
Qiu Q, Sayer M, Kawaja M, Shen X, Davies JE (1998) Attachment, morphology, and protein expression of rat marrow stromal cells cultured on charged substrate surfaces. J Biomed Mater Res 42: 117–127
Raiteri R, Martinoia S, Grattarola M (1996) pH-dependent charge density at the insulator-electrolyte interface probed by a scanning force microscope. Biosens Bioelectron 11: 1009–1017
Raiteri R, Margesin B, Grattarola M (1998) An atomic force microscope estimation of the point of zero charge of silicon insulators. Sens Actuators B 46: 126–132
Rajnicek AM, Robinson KR, McCaig CD (1998) The direction of neurite growth in a weak DC electric field depends on the substratum: contributions of adhesivity and net surface charge. Dev Biol 203: 412–423
Rich A, Harris AK (1981) Anomalous preferences of cultured macrophages for hydrophobic and roughened substrata. J Cell Sci 50: 1–7
Richards RG (1996) The effect of surface roughness on fibroblast adhesion in vitro. Injury 27: SC38–SC43
Rumpel E, Behrends JC (1999) Evoked asynchronous transmission rat striatal inhibitory synapses. J Physiol (Lond) 514: 447–458
Schottelndreier H, Mayr GW, Guse AH (1999) Beta1-integrins mediate $Ca^{2+}$-signalling and T cell spreading via divergent pathways. Cell Signal 11: 611–619
Sebben M, Gabrion J, Manzoni O, Sladeczek F, Gril C, Bockaert J, Dumuis A (1990) Establishment of a long-term primary culture of striatal neurons. Dev Brain Res 52: 229–239
Singhvi R, Stephanopoulos G, Wang DIC (1994) Review: effects of substratum morphology on cell physiology. Biotechnol Bioeng 43: 764–771
Smit W, Holten CLM (1980) Zeta-potential and radiotracer adsorption measurements on EFG $\alpha$-$Al_2O_3$ single crystals in NaBr solutions. J Colloid Interface Sci 78: 1–14
Soekarno A, Lom B, Hockberger PE (1993) Pathfinding by neuroblastoma cells in culture is directed by preferential adhesion to positively charged surfaces. Neuroimage 1: 129–144
Stetefeld J, Mayer U, Timpl R, Huber R (1996) Crystal structure of three consecutive laminin-type epidermal growth factor-like (Le) modules of laminin gamma1 chain harboring the nidogen binding site. J Mol Biol 257: 644
Tanzer ML, Chandrasekaran S, Dean JW, Giniger MS (1993) Role of laminin carbohydrates on cellular interactions. Kidney Int 43: 66–72
Torimitsu K, Kawana A (1990) Selective growth of sensory nerve fibers on metal oxide patterns in culture. Dev Brain Res 51: 128–131
Tryggvason K (1993) The laminin family. Curr Opin Cell Biol 5: 877–882
Vassanelli S, Fromherz P (1998) Transistor-records of excitable neurons from rat brain. Appl Phys A 66: 459–463
Weiss S, Pin JP, Sebben M, Kemp DE, Sladeczek F, Gabrion J, Bockaert J (1986) Synaptogenesis of cultured striatal neurons in serum-free medium: a morphological and biochemical study. Proc Natl Acad Sci USA 83: 2238–2242
Wu RL, Barish ME (1994) Astroglial modulation of transient potassium current development in cultured mouse hippocampal neurons. J Neurosci 14: 1677–1687
Yon E, Ko WH, Kuper AB (1966) Sodium distribution in thermal oxide on silicon by radiomechanical and MOS analysis. IEEE Trans Electron Devices 13: 276–280
Zhmud BV, Meurk A, Bergström L (1998) Evaluation of surface ionization parameters from AFM data. J Colloid Interface Sci 207: 332–343